Energy Management Research Journal
Vol. 2, No. 1; 2019
Published by CanSRG
http://cansrg.com/journals/emrj/

Combined Exploitation of Onshore Wind-Wave Energy in the Niger Delta Coasts Based on a 37-year Hindcast Information

Osinowo Adekunle Ayodotun

Department of Marine Science and Technology, Federal University of Technology, Akure, Nigeria

Abstract

This study presents results from an investigation of combined wind-wave energy resources over the Niger delta coasts by using the significant wave height (SWH) and mean wave period (Tm) data spanning a 37 year (1980-2015) period and derived from the analysis of wave climate predictions generated by the WAVEWATCH-III (WW3) wind-wave model. Analysis showed that there are no rich wave energy regions and the wind generally showed very poor characteristics (WPD of 33.44 w/m^2). Hence, the region is poor for large-scale wind power applications and not suitable for the exploitation of wave energy and in the establishment and design of wave energy converter systems. The monthly wind analysis revealed that the wind is strongest, most stable and most spread in August with respective values of 4.3m/s, 4.97 and 4.68m/s. Seasonal analysis showed that the wind is stronger, more stable and more spread in summer, winter and summer with respective values of 3.43m/s, 3.31 and 3.83m/s. The wind power density (WPD) and wave power density (WVPD) intensified westwards with maximum values of 70-86.5w/m^2 and 0.5-0.61kW/m found around Gulf of Guinea. The WPD and WVPD generally showed declining trends for the year and seasons. The wave power is minimum in the year 1999 respectively for the annual, winter and summer averages of 0.04kW/m. Wave power stability intensifies westwards. It is most stable (1.1-1.2) around Lagos Lagoon and least stable (1.5-1.62) around Ikpa Ibom IV. The wave power stability generally showed declining trends. Furthermore, the analysis of both the monthly variability index (MVI) and seasonal variability index (SVI) showed that wave power stability increases west wards. The greatest stability (0.96-2.3) is seen around Lagos Lagoon and southwards towards the western Gulf of Guinea. It is least stable (1.14-2.79) in Ikpa Ibom IV. For the MVI and SVI, temporal variation showed that the wave power is most stable in the year 1999 with respectively values of 0.33 and 0.07. The bivariate distribution of SWH and Tm revealed that the most frequent sea states coincide with the most energetic sea states.

Keywords: *Wave Power; Trend; Distribution; Region; Variation; Occurrence.*

1. Introduction

The attention given to the harnessment of the renewable energy resources has increased considerably in the past years. The oceanic environment represents a vast source of renewable energy and has a great potential for the development of the renewable energy projects. The ocean resources characterized by the tidal currents with ocean surface waves are clean energy resources having excellent potentials over enlarged areas [1-5]. However, harnessing the wind energy is as well feasible in these locations but the establishment and maintenance expenditures of the offshore wind farms are higher [6]. A chance to thwart this weakness and to compensate large expenses could be to encourage the use of a combined harnessment of the wind-wave energy

Submitted: September 12, 2019 Accepted: December 21, 2019

resources either by using hybrid devices or co-located wind-wave farms [7-8]. [9-10] are studies relevant to hybrid marine energy projects. Assessment of the wind-wave energy potential have been carried out in various locations in the universe [11], but only a few works highlighted the complementarities of both resources for combined utilization. Current work related to the combined exploitation of the offshore waves and wind energy show that this is a promising choice in several regions of Europe [12-15] or elsewhere in the globe [16]. Along with this, some studies estimated the combination of these resources and how they work with each other to improve economic competitiveness.

Ocean renewable energy infrastructures could add to the future energy power supply [17]. The wind energy from the oceanic environment is the most developed kind in the midst of the various developed marine renewable technologies with respect to technological development, commercialization, policy frameworks, and installed capacity [18-19]. Really, most of the concern is based on the improvement of fresh offshore solution, like wind turbines with bigger rotors, deep water locations and floating platform (e.g., Hywind Scotland project www.statoil.com) [20]. Floating technology can be regarded as a commercially feasible solution just to exploit accessible wind resource also at larger depth (>50 m) where the usual fixed offshore wind turbines are no more financially viable [21]. Wave Energy Converters (WECs) have been noted as machinery with the prospect to represent an excellent role in the medium to long term [22]. Universally, in 2017 wave energy deployments have increased its capacity respect to the preceding year, up to 8 MW [17].

The viability of merging a floating wind turbine and a wave energy converter has been examined by various authors [23, 24-29]. Wind-wave technology is a long lasting solution to lessen the intermittence of the wind-wave resources irrespective of the time interval, growing in this manner the goodness of a location in respect of its total marine energy potential [23, 30-31, 20]. Therefore, the diversification of the combined renewable energy technologies, decides a lessening of the power's variability [16, 23] and the energy expenditures [32-34].

The choice to join wind-wave energy technologies have been carried out for the Mediterranean location by [35]. Precisely and in accordance to the ORECCA1 project results, the Mediterranean appropriate regions are majorly limited to three probable regions: the Blue Coast (southern France coast), the Aegean Greek islands and the strait of Sicily (between Sicily and Tunisia). In current years, the potential oceanic regional effects of renewable energy tools have been described in various researches [36-38].

Over the Mediterranean location, there are areas where wind-wave energy showed low, but not insignificant mean values. Rich regions for combined exploitation are found in the Gulf of Lions, Sicily Straits (Central Mediterranean), off the coasts of Sardinia, off the NE coasts of the Balearic Islands (NW Mediterranean) and in identified locations in the Aegean Sea.

At present, little or no studies have been carried out on wind-wave energy potential in the Niger delta coasts. This study therefore evaluates the potential of wind and wave energy and to estimate areas viable for combined exploitation of both resources over the region. These attributes of the renewable resources are analyzed in the present study using reanalysis data for the wind conditions and hindcast simulations of the sea states. Furthermore, the bivariate distribution of wave energy will be analyzed and investigation will be made to identify sites of relative rich wave energy, ideal for the installation of wave power plants for electrical energy generation.

This work is organized as follows. Section 2 provides details about the model configuration, the wind field data and validation tests of model data with buoy data for the Significant wave height, mean wave period and 10m wind speed. The analytical methods used in evaluating wind and wave power in the Niger delta coasts followed by results and discussion are all presented in section 3. Finally, section 4 concludes the work.

2. Models, Data Sets and Data Validation

2.1. The Wave Model and Input Data

Six hourly averaged ocean wave parameters such as significant wave height, wave direction, mean and peak wave period were simulated over the mid-Atlantic Ocean by using the version 3.14 of the third-generation spectral wave model i.e. Wavewatch 3 model (WW3). The wave model also outputs 10 m wind speed. It was built up at the Ocean Modeling Branch of the Environmental Modeling Center of the National Center for Environmental Prediction (NCEP) for ocean wave forecasts. It was developed from Wavewatch-I and Wavewatch-II at the Delft University of Technology, and NASA Goddard Space Flight Center, respectively [39]. By using the National Geophysical Data Center (NGDC) one minute Bathymetric, Topographic/Elevation (ETOP 01) data, with a resolution of 0.017 ° × 0.017 °, the water depth field over the mid-Atlantic ocean defined by coordinates 58°W, 8°S, 18°E and 18°N and which was processed by the Gridgen 3.0 packet was obtained.

The model spatial grid covers a large part of the mid-Atlantic Ocean with coordinates 58^{o}W to 18^{o}E and 8^{o}S to 18^{o}N at a resolution of 0.083^{o}. The model uses a time step of 3600 s which was forced with six hour re-analysis wind fields (zonal (u10) and meridional (v10) and extracted over 60^{o}W to 20^{o}E and 10^{o}S to 10^{o}N from the ECMWF, ERA-Interim. The wind data spans from 1st January 1980 to 31st December, 2015 on a 0.125^{o} by 0.125^{o} Gaussian grid. The model output is a two-dimensional (2D) wave energy spectra got at each grid point. The simulation provided a time series of wind and wave parameters over a box extending from 58^{o}W to 18^{o}E and 8^{o}S to 18^{o}N, which contains onshore and offshore locations. A MATLAB program was written to extract results over the Niger delta coasts bounded by 3-8°E and 4-6.5°N (Figure 1).

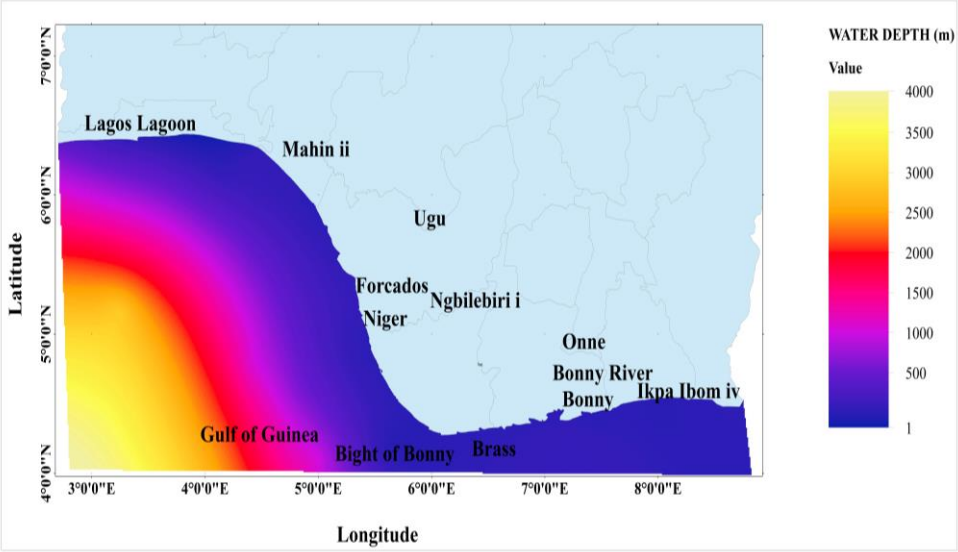

Figure 1. Topography of Niger delta coasts and surrounding waters.

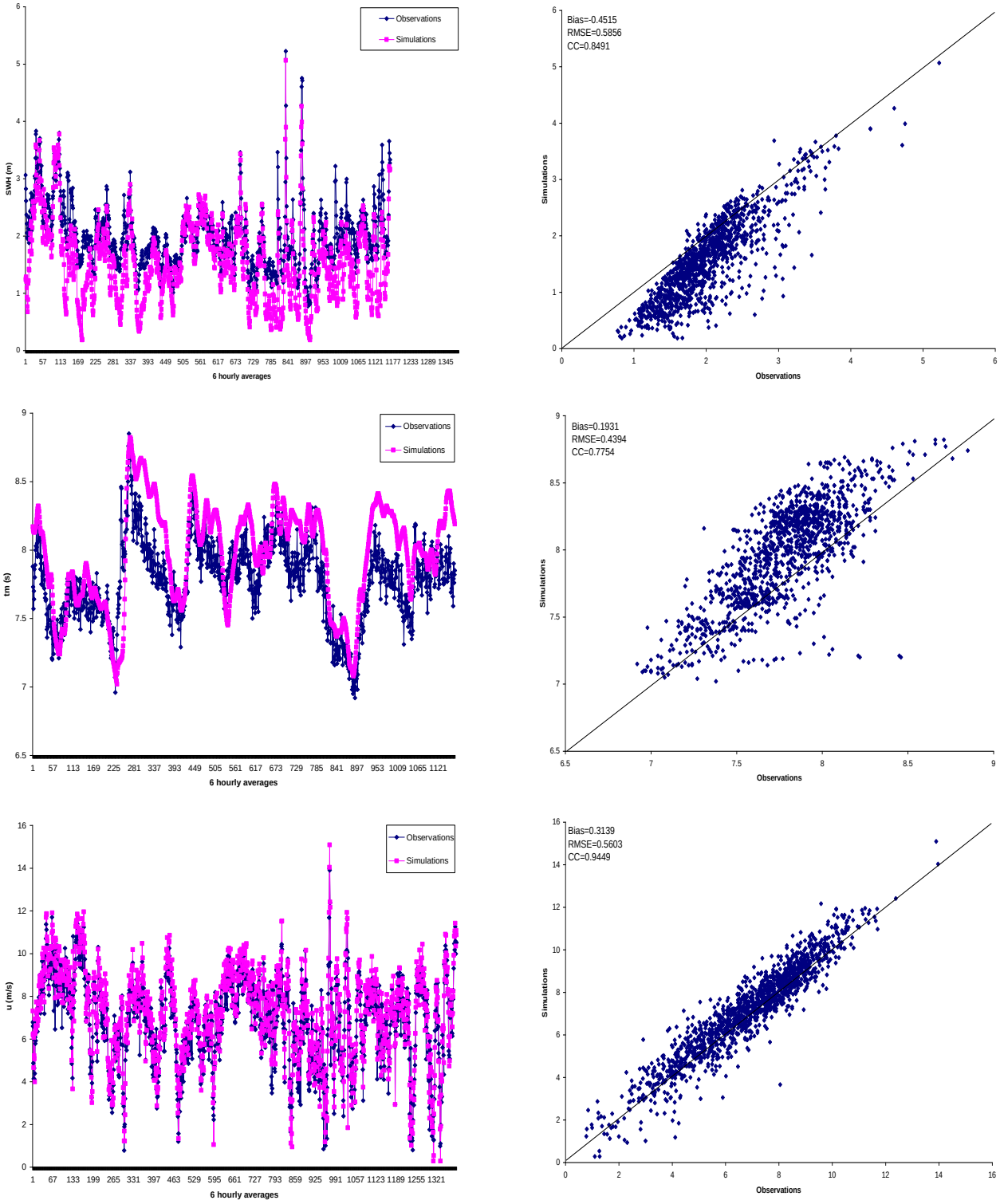

(a) (b)

Figure 2 (a) Time-series and (b) scatter plots of the model data against buoy data (6-hourly averages) for significant wave height, mean wave period and wind speed for the period 1 January to 31 December 2011. The fitted line in (b) represents a difference of zero and indicates the degree of underestimation or overestimation of modeled data. Bias = mean bias error; RMSE = root mean square error; *cc* = correlation coefficient. On the x-axis is the number of data points.

2.2. Data Validation

The Buoy (observational) data was obtained from the National Data Buoy Center (NDBC) for buoy 41040 3D56/AR in NORTH EQUATORIAL ONE, coordinates 14.516N, 53.024W which is an observation station in the mid-Atlantic.

Figure. 2 shows the comparisons conducted between observations and simulations for the SWH, Tm and u for year 2011. The corresponding parameters were computed by the model over the buoy coordinates. There is good agreement between observations and simulations on the curve trends.

The accuracy of the wave parameters and wind computed by the model was evaluated through a conventional statistical analysis that consists of calculating the following in [40]:

$$cc = \frac{\sum_{i-1}^{n}(x_i - \bar{x})(y_i - \bar{y})}{\sqrt{\sum_{i-1}^{n}(x_i - \bar{x})^2 \sum_{i-1}^{n}(y_i - \bar{y})^2}} \quad (1)$$

$$Bias = \bar{y} - \bar{x} \quad (2)$$

$$RMSE = \sqrt{\frac{1}{N}\sum_{i-1}^{n}(y_i - x_i)^2} \quad (3)$$

where, x_i represents the buoy data, y_i represents the model data, x and y are the mean values of buoy and model data and N is the total number of observations.

As shown in Figure 2(b), it is clear that the significant wave height, mean wave period and 10m wind speed computed by the model and their observed values are highly correlative with respective correlation coefficients (cc) of 0.8491, 0.7754, 0.9449 and significant at the 99% level. The calculated mean bias error (MBE) of -0.4515 m, 0.1931s and 0.3139 m/s respectively for the significant wave height, mean wave period and 10m wind speed showed that the model data slightly underestimates the buoy data except for the significant wave height in which the model data slightly overestimates the buoy data. The root mean square errors (RMSE) of model data for the Significant wave height, mean wave period and 10 m wind speed are respectively 0.5856 m, 0.4394 s and 0.5603 m/s.

In general, the simulation results are consistent with the observations, which show that WW3 serves as a reliable model and can well reproduce these wind-wave parameters in the Nigerian coasts.

3. Analysis Methods

3.1. Computation of Wind Energy

For years, models like Rayleigh, Weibull, log-normal, and normal, were engaged in wind data analysis [41]. The two-parameter Weibull probability distribution function is widely recommended for wind data evaluation because it agrees with experimental data [42]. The model is on the whole, a gamma function that calculates the WPD and depicts the wind speed frequency distribution [43]. Therefore, this study employed the two-parameter Weibull distribution function to compute WPD.

The Weibull probability density function is expressed in [43] as

$$f(v) = \frac{k}{c}\left(\frac{v}{c}\right)^{k-1} \exp\left[-\left(\frac{v}{c}\right)^{k}\right] \quad (4)$$

The matching cumulative density function is expressed in [43] as

$$F(v) = 1 - \exp\left[-\left(\frac{v}{c}\right)^{k}\right] \tag{5}$$

The shape and scale parameters are respectively k and c; v is the wind speed; k which is dimensionless, stands for the variation in the average wind speed in a given sample; and c in m/s depicts the wind potential over a region which is computed using different methods, like standard deviation (STD) method [44], power density method [45], maximum likelihood method [46] and graphical method [47]. The higher the value of "k" , the more stable the wind is. The higher the value of "c", the more spread is the wind power [48]. This work utilized the STD technique, which is expressed in [44, 49] as

$$k = -\left(\frac{\sigma}{\bar{v}}\right)^{-1.086} \qquad \text{for } 1 \le k \le 10 \tag{6}$$

$$c = \frac{\bar{v}}{\Gamma\left(1+1/k\right)} \tag{7}$$

where $\bar{v}$ is the mean wind speed (m/s), and σ is the STD that explains the degree of deviation of the wind speed. Γ(x) is the gamma function expressed in [50] as

$$\Gamma(x) = \int_0^{\infty} \exp(-u)\, u^{x-1} dx \tag{8}$$

WPD is expressed in [51] as:

$$P_d = \frac{P(v)}{A} = \frac{1}{2}\rho \int_0^{\infty} v^3 f(v)\, dv = \frac{1}{2}\rho c^3 \Gamma\left(1+\frac{3}{k}\right) \tag{9}$$

where P_d is the WPD in units of w/m^2, P (v) denotes the wind power in watts, A is the swept area of the wind turbine rotor in units of w/m^2, and ρ denotes the air density which is assumed to be 1.225 kg/m^3.

3.2. Evaluation of Wave Power

By using the evaluation method of [2, 52-53], the WVPD is estimated as follows

$$P_w = \frac{\rho g^2}{64\Pi} H^2_{mo} T_e = 0.49 H^2_{mo} T_e \tag{10}$$

where P_w is wave power (kW/m), H_{mo} is the significant wave height (unit: m), and T_e is the mean wave period (s).

The distribution in relative rich energy of the WVPD is determined. [54] suppose the region with seasonal average WVPD above 6kW/m and coefficient of variation (COV) below 2.0 as the relative rich-energy region. This is adopted in this study.

Many measures can be conceived to describe the variability in wave power at a site. One simple, straightforward measure is the COV. The wave power stability is evaluated by calculating the COV for each grid point. The lesser the COV, the more the stability.

The COV calculating formula is as follows.

$$COV = \frac{s}{\bar{x}} \tag{11}$$

where s is the STD and is evaluated as

$$S = \sqrt{\frac{\sum_{i=1}^{n} x_i^2 - (\sum_{i=1}^{n} x_i)^2/n}{n-1}} \quad (12)$$

The seasonal variability index (SVI), is expressed as

$$SVI = \left(P_S 1 - P_S 4\right) \Big/ Pyear \quad (13)$$

and the monthly variability index (MVI) is expressed as

$$MVI = \left(P_M 1 - P_M 12\right) \Big/ Pyear \quad (14)$$

Where *P*s1 and *P*s4 are respectively the maximum and minimum seasonal mean WVPD, P_M1 and P_M12 are respectively the maximum and minimum monthly mean WVPD and *P*year is the annual mean WVPD. Higher index values indicate larger wave energy variations and decreased stability compared with lower index values.

By using wave height and wave period at defined intervals of 2.5 m and 2.5 s, the bivariate distribution of occurrence and total wave power were analyzed for the Niger delta coast.

In this work, the wind speed data for 1980-2015 were statistically evaluated. The frequency distribution, monthly and seasonal variations in the Weibull parameters, WPD and mean wind speed were obtained. Also, the monthly and seasonal values of the wind STD, wind COV, WPD ratio and wind speed ratio were determined. The spatio-temporal characteristics of WPD, WVPD, wave power stability and the monthly with the seasonal variability index of wave power were evaluated. The relative rich energy regions in WVPD were determined.

3.3. Results and discussion

3.3.1. Wind Characteristics

The monthly variation of wind and their annual mean values are presented in Table. 1. The shape parameter "k" varies between 3.13 and 4.97 in October and August respectively, which reveals that the wind data is most stable in the month of August and least stable in October. Consequently, August is appropriate for the production of incessant and stable wind power. The scale parameter "c" ranges between 2.67 m/s and 4.68 m/s in November and August respectively, indicating that the wind power is most spread in August and least spread in November. The monthly mean wind speed varies between 2.4 m/s in November and 4.30 m/s in August. The WPD ranges between 13.98 w/m^2 in November and 70.61 w/m^2 in August. The STD of the wind is highest (1.21) in July and lowest (0.85) in November. The wind is most stable (COV 26.43%) in August and least stable (COV 36.87%) in October. The annual mean WPD and wind speed stand at 33.44 w/m^2 and 3.14 m/s respectively.

Table 2 shows the seasonal variation of wind. For the weibull parameters, the shape and scale parameters respectively show that the wind is more stable (3.31) in winter and more spread (3.83 m/s) during summer. Higher values of both the WPD and u are observed in summer with respective values of 42.66 w/m^2 and 3.43 m/s. The wind STD is higher (1.23) during summer while the wind is more stable (35.66%) during winter.

For the wind power classification proposed by [55] of Pacific Northwest Laboratory (Table 3), the annual mean WPD for the Niger delta coasts (33.44w/m^2) is categorized as class 1, which indicates that the region is poor for large scale wind power applications. The wind potential of

the region can be adequate for non-grid connected electrical and mechanical applications, such as wind generators, battery charging and water pumping as well as agricultural applications.

Table 1. Monthly and Annual Mean Wind Characteristics.

Month	k	c (m/s)	WPD (w/m^2)	u (m/s)	STD	COV (%)
Jan	3.19	2.96	18.80	2.65	0.97	36.28
Feb	3.56	3.33	26.47	3.00	0.98	32.45
Mar	3.66	3.43	29.13	3.10	0.97	31.40
Apr	3.50	3.28	25.59	2.96	0.95	32.31
May	3.22	3.10	22.44	2.79	0.98	35.16
Jun	3.34	3.77	41.76	3.40	1.20	35.89
Jul	4.20	4.55	67.98	4.15	1.21	30.41
Aug	4.97	4.68	70.61	4.30	1.08	26.43
Sep	4.15	4.02	47.26	3.67	1.05	29.86
Oct	3.13	3.07	22.81	2.76	1.01	36.87
Nov	3.18	2.67	13.98	2.40	0.85	35.46
Dec	3.31	2.73	14.42	2.45	0.87	35.29
Annual	3.62	3.47	33.44	3.14	1.01	33.15

Table 2. Seasonal Mean Wind Characteristics.

Season	k	c (m/s)	WPD (w/m^2)	u (m/s)	STD	COV (%)
Winter	3.31	3.04	20.44	2.72	0.97	35.66
Summer	3.06	3.83	42.66	3.43	1.23	36.45

Table 3. Wind power classification [55].

Power Class	Power density (w/m^2) at 10 m
1	$0 < P \leq 100$
2	$100 < P \leq 150$
3	$150 < P \leq 200$
4	$200 < P \leq 250$
5	$250 < P \leq 300$
6	$300 < P \leq 400$
7	$400 < P \leq 1000$

Figures 3a and b present the monthly and seasonal variations of the WPD ratio and u ratio. For both wind variables in figure IIIa, the ratio is highest in August with respective values of 2.11 and 1.37 and least in November with respective values of 0.42 and 0.77. For the seasons in figure 3b, higher values of 1.35 and 1.12 are observed during summer.

The percentage frequency distribution of wind speed is shown in figure 4. The wind speed within the range of 0-4 m/s has the highest frequency of 73.94 % while the wind speed in the range of 12-16 m/s has the lowest frequency of 0.000761%.

3.3.2. Relative Rich Energy Regions and Spatio-temporal Characteristics of WPD

This section highlights the regional variation in relative rich energy with the distribution and temporal trends of WPD in the Niger delta coasts. As shown in figure 5a, the wave power is

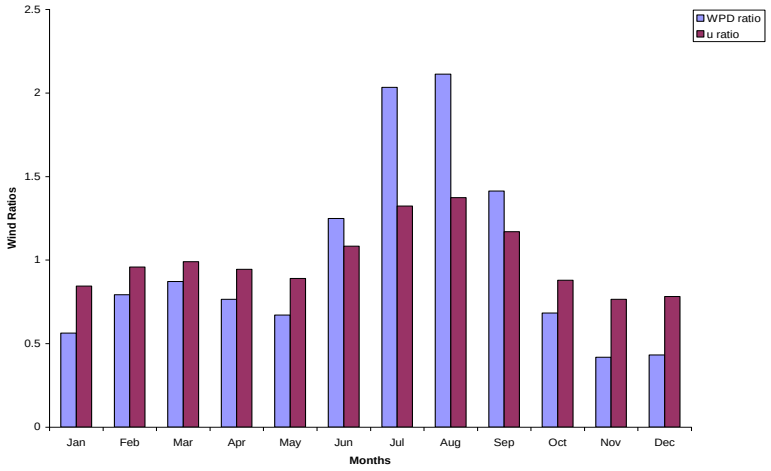

Figure 3(a). Monthly variation in the wind ratios.

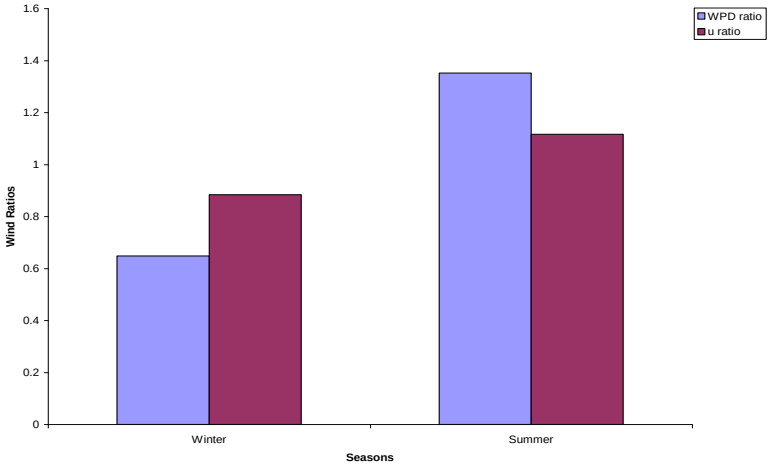

Figure 3(b). Seasonal variation in the wind ratios.

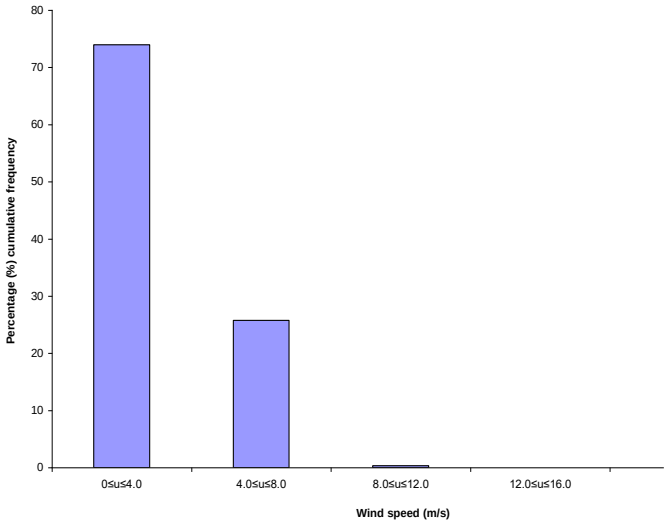

Figure 4. The percentage frequency distribution of wind speed obtained from the thirty six years (1980-2015) daily average wind speed data over the Niger delta coast.

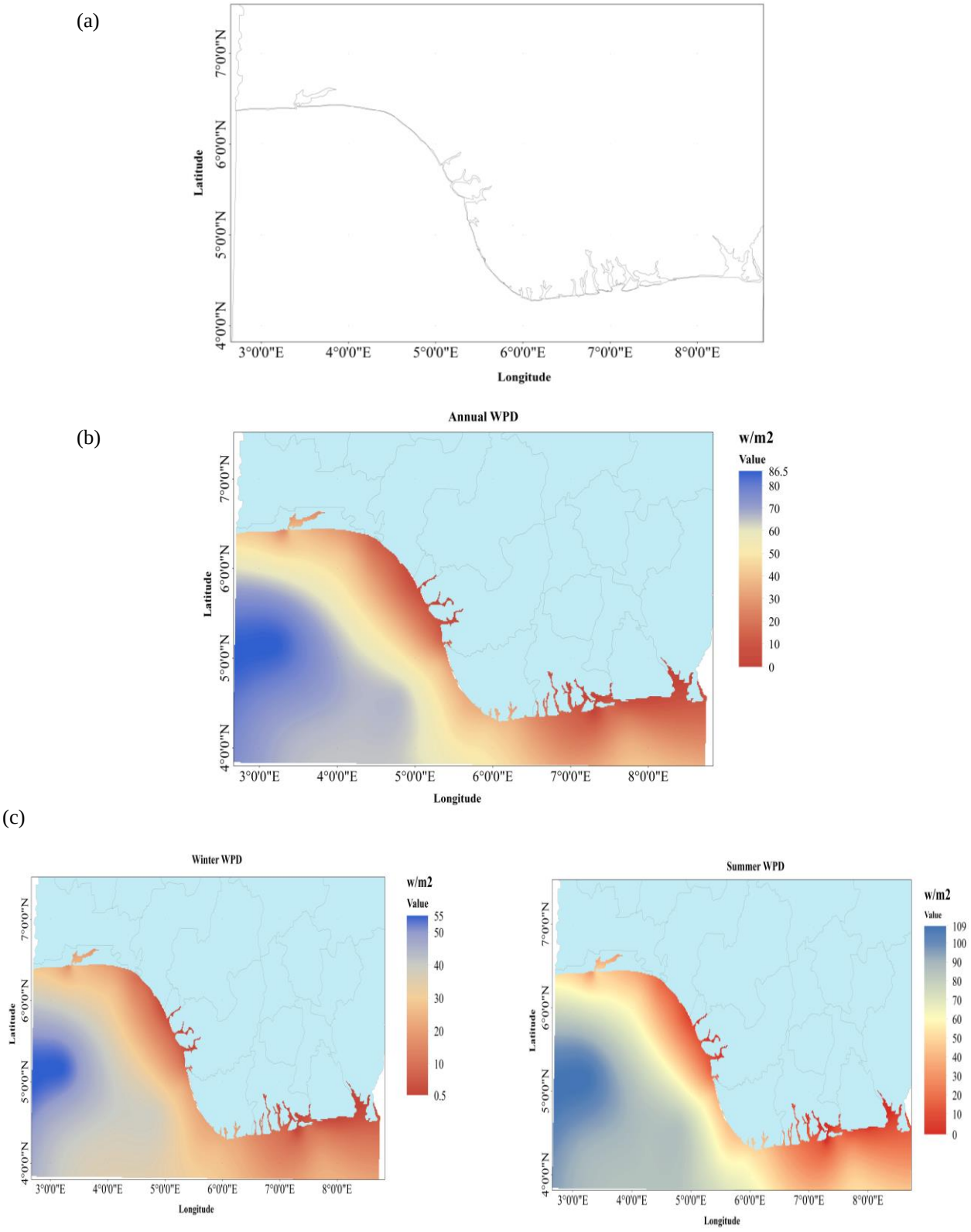

Figure 5. (a) Wave power in relative rich-energy regions, (b) annual and (c) seasonal distribution of WPD for the period 1980-2015.

relatively poor in all parts of the Niger delta coasts but ordinary wave energy is only available. The poor wave power in these regions is due to very low wind speeds, which has little influence on sea states of waves. Therefore, the Niger delta coasts are not ideal for the installation of wave power plants for massive electrical energy generation. The annual average distribution of WPD is as shown in figure 5b. WPD intensifies westwards with peak values ($70w/m^2$ - $86.5w/m^2$) distributed around Gulf of Guinea. Values ranging between $50w/m^2$ and $60w/m^2$ centre around Lagos Lagoon. Least values (< $20w/m^2$) are found in the onshore regions such as Mahin II, Forcados, Niger, Brass, Bonny and Ikpa Ibom IV. For the seasons in figure. 5c, larger values of WPD are generally observed in summer than during winter. At winter, maximum values ($50w/m^2$ - $55w/m^2$) distribute in the northwestern Gulf of Guinea. Values between $30w/m^2$ and $40w/m^2$ dominate the central Gulf of Guinea while values below $20w/m^2$ distribute in the rest region. Also, during summer, WPD is largest ($100w/m^2$ - $110w/m^2$) in the northwestern Gulf of Guinea. The values decrease eastwards and minimum (< $20w/m^2$) along the coasts of Mahin II, Forcados, Niger, Brass, Bonny and Ikpa Ibom IV.

The general long-term trends in the annual and seasonal mean wind power analyzed by using linear regression method with a reliability test of 95% are shown in figure 6. The yearly and seasonal average wind power was determined by calculating the regional mean wind power from 00:00 UTC on January 1, 1980 to 18:00 UTC on December 31, 2015. The WPD generally showed declining trends for the year and seasons. The annual trend is -0.0021 w/m^2yr^{-1} while the trends at winter and summer are respectively -0.2107 w/m^2yr^{-1} and -0.362 w/m^2yr^{-1}. For the annual and summer averages, the WPD is minimum in the year 1999 with respective values of $18.71w/m^2$ and $18.98w/m^2$ while largest values of $44.53w/m^2$ and $60.35w/m^2$ are found in the year 1981. For the winter average, highest WPD values of $25.1w/m^2$ and $23.9w/m^2$ are respectively found in the years 1983 and 1992 while least values of $15.9w/m^2$ and $16.3w/m^2$ are respectively found in the years 1995 and 1997.

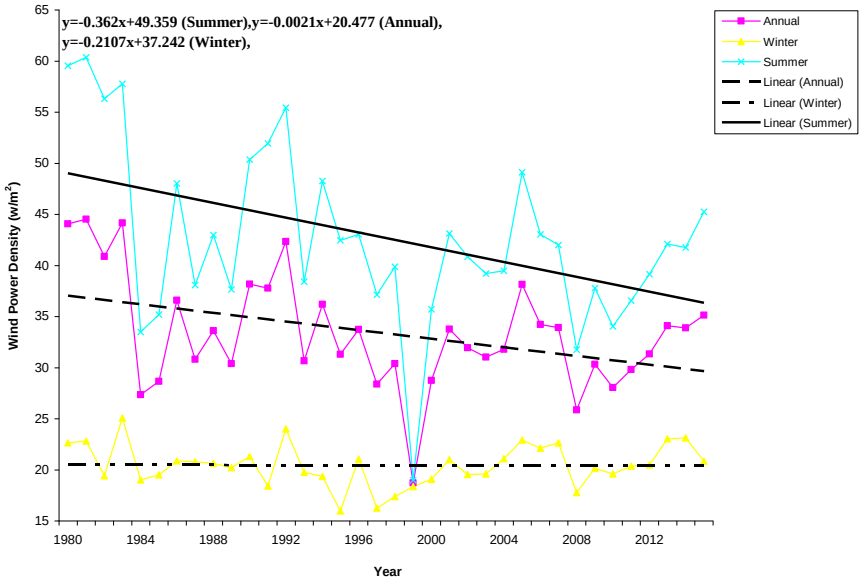

Figure 6. Annual and seasonal temporal trends in WPD for the period 1980-2015 over the Niger delta coasts, unit: w/m^2yr^{-1}.

3.3.3. Spatio-temporal Characteristics of WVPD

The regional distribution of annual and seasonal mean WVPD derived from analysis of the WW3-Niger delta wave climatology are presented in figures 7a and b. In figure. 7a, the yearly average wave power in the range of 0.3kW/m - 0.61kW/m dominate most waters of the Niger delta. Lower values (0.2kW/m - 0.29kW/m) are observed around the Lagos Lagoon and in waters surrounding Bight of Bonny and Brass. Values below 0.2kW/m occur around Ikpa Ibom IV. In figure 7b, the distribution during winter shows that wave power between 0.2kW/m and 0.23 kW/m occupy a large portion of the ocean and it is particularly strongest (~ 0.23 kW/m) in the central Gulf of Guinea. Values between 0.1kW/m and 0.16kW/m occur around Lagos Lagoon, Brass and Bight of Bonny. Least values (<0.05 kW/m) occur around Ikpa Ibom IV. During summer, wave power values between 0.7kW/m and 0.88kW/m distribute in a large part of the ocean but more intensified (~ 0.88 kW/m) in the northwestern Gulf of Guinea. Lower values (0.3kW/m - 0.6kW/m) are found around Lagos Lagoon, Mahin II, Forcados, Niger, Bight of Bonny and waters to its east. Minimum values of less than 0.2kW/m are seen in waters on the coast of Bonny and Ikpa Ibom IV.

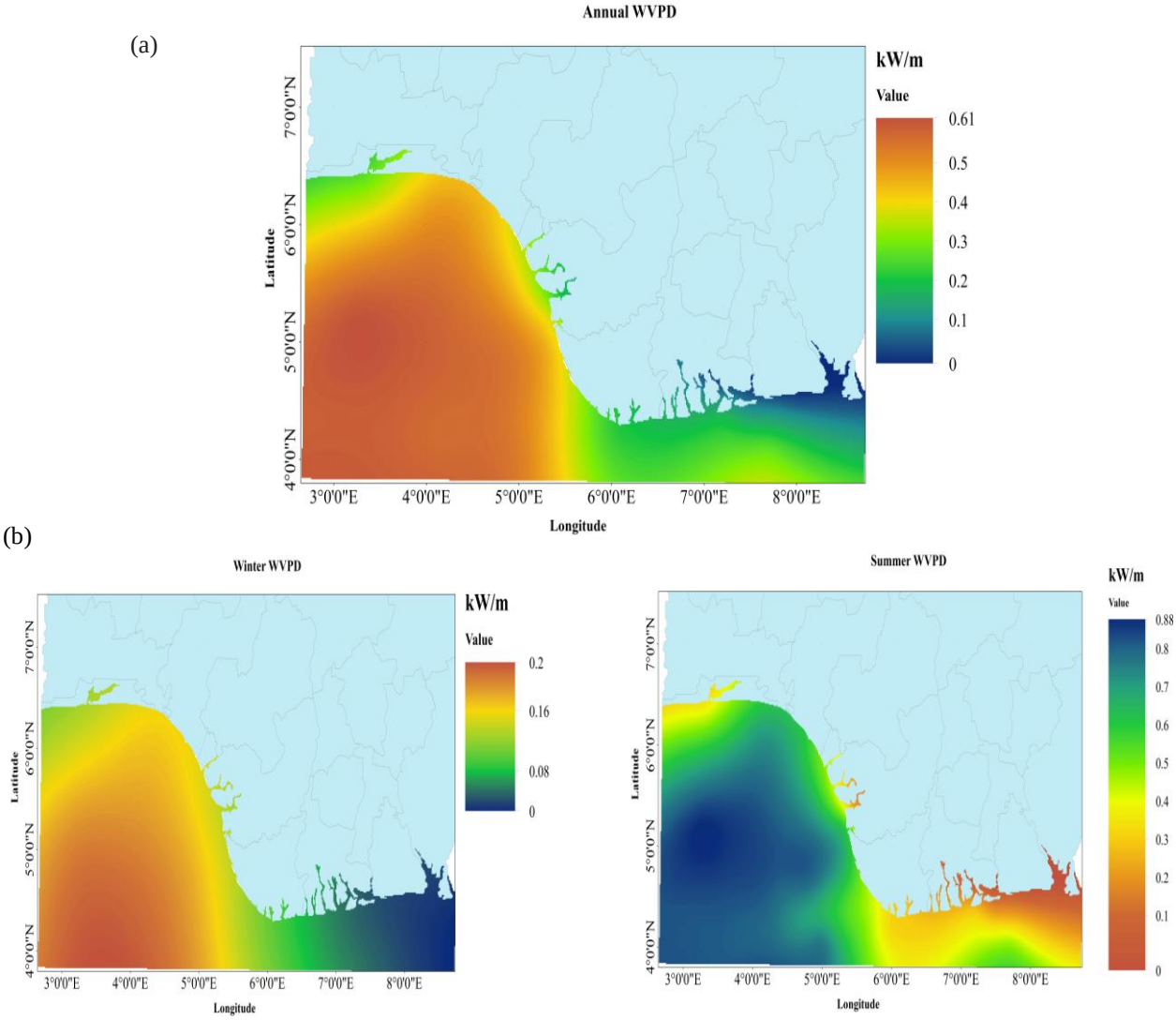

Figure 7. (a) annual and (b) seasonal mean WVPD in the Niger delta coasts.

The analysis of wave power distribution is of high relevance to researchers who work on the development of wave energy converter, as it provides information on sites suitable for the installment of wave energy converters (WECS). It is therefore recommended that the northwestern Gulf of Guinea is more suitable for the installation of WECS at least for a domestic supply of electricity.

The long-term temporal trends of the annual and seasonal mean wave power over the Niger delta coasts are presented in figure 8. For the year and seasons, the wave power generally exhibits declining trends. The annual trend is -0.0029kW/myr^{-1} while the trends at winter and summer are respectively -0.0003 kW/myr^{-1} and -0.0048 kW/myr^{-1}. The wave power is minimum in the year 1999 with respective values of 0.039 kW/m and 0.038 kW/m for both the annual and summer averages. Largest wave power of 0.45 kW/m and 0.67 kW/m are seen in the year 1991. For the winter mean, highest wave power values of 0.16 kW/m, 0.15 kW/m, 0.16 kW/m and 0.17 kW/m are respectively found in the years 1980, 1988, 1992 and 2014, while least value of 0.04 kW/m is found in the year 1999. The declining trends can be generally adduced to insignificant influences of storminess, atmospheric circulation and monsoonal variation. Between years 1998 and 2000, the abrupt fall and rise in wave power is associated with hurricane intensity and storminess in the basin, accompanying the weakening and strengthening of the West African Monsoon.

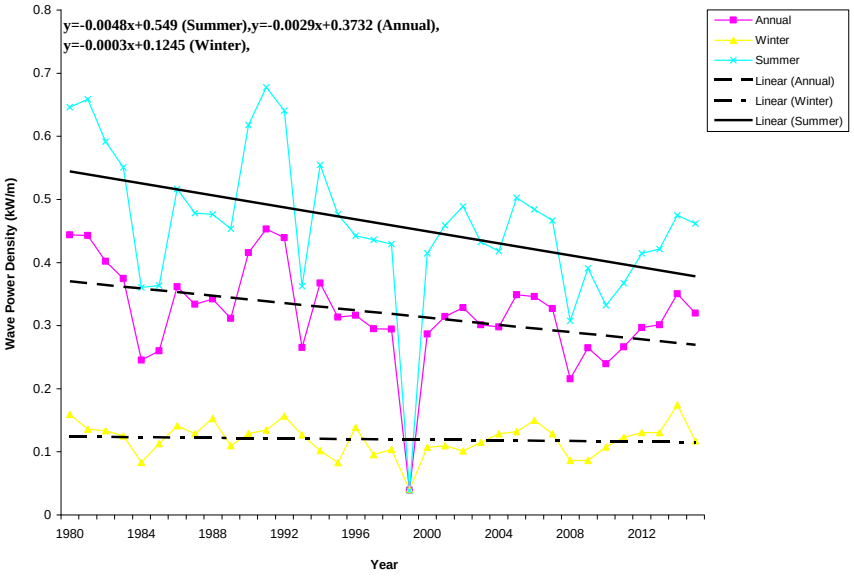

Figure 8. Annual and seasonal temporal trends in WVPD for the period 1980-2015 over the Niger delta coasts, unit: kW/myr^{-1}.

3.3.4. Spatio-Temporal Variation in Wave Power Stability

Cornett [2] found that wave power stability affects the feasibility of wave energy resource harnessment projects in any marine environment. Wave power stability is more germane than the wave power resource and stable wave power is excellent for use. The stability in wave power is defined by COV, MVI and SVI. Higher values denote larger wave energy variations and lower stability as compared to lower values.

The annual and seasonal stability of the wave power together with the temporal trends are all shown in figures. 9 and 10. Considering the annual and seasonal mean wave power stability presented in figure 9, the stability in wave power generally increases westwards and it is most

stable (COV of 1-1.1) around Lagos Lagoon. The wave power has the largest variation and least stable (COV of 1.25-1.65) around Ikpa Ibom IV. The eastward decrease in wave power stability is due to the dramatic changes in wave height caused by tropical cyclones and the seasonal variation in stability resulted from monsoonal influence. In general, the stability is more pronounced in the offshore than in the near shore locations of the Ocean. This is due to the relatively regular and stable ocean waves caused by incessant blast of cold air in the offshore locations of the Niger delta.

(a)

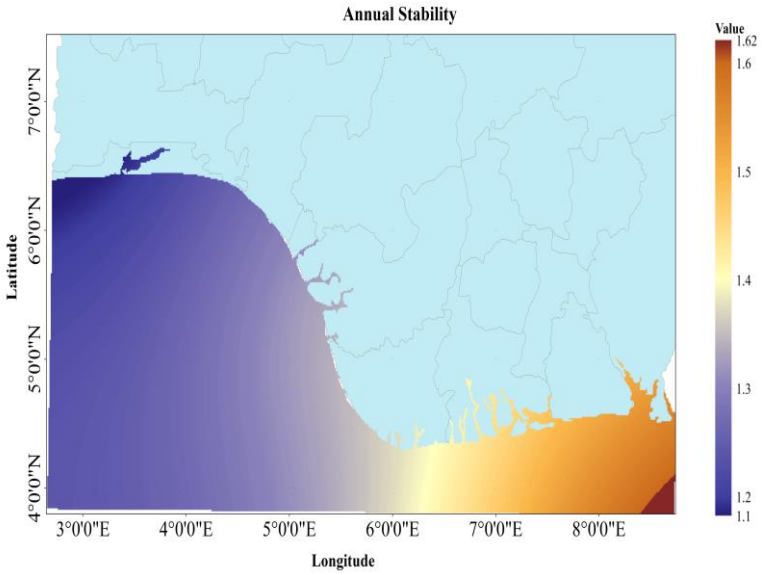

(b)

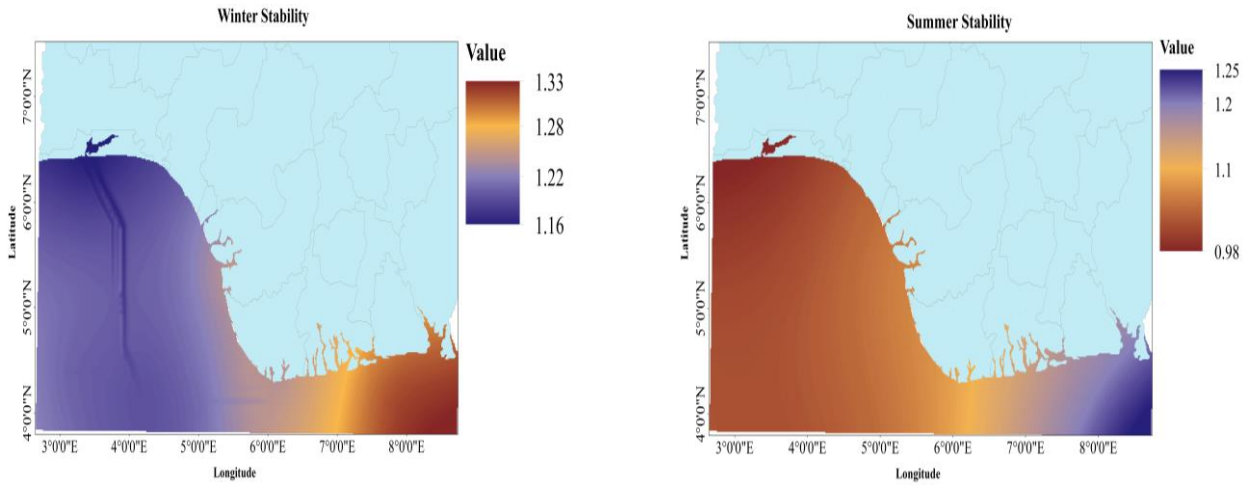

Figure 9. (a) annual and (b) seasonal stability of wave power in the Niger delta coast.

In figure. 10, the wave power stability exhibits declining trends of -0.0017, -0.0064 and -0.00008 respectively for the annual, winter and summer averages. The wave power is most stable in the year 1999 with COV ranging between 0.011 and 0.51 in all the three cases.

The monthly and seasonal variability indexes of wave power are presented in figure. 11 while their temporal variations are displayed in figure. 12.

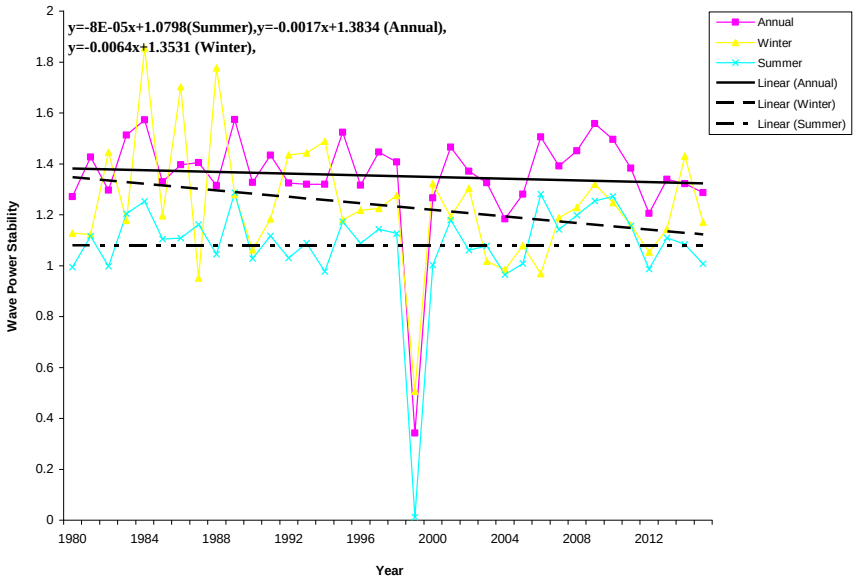

Figure 10. (a) annual and (b) seasonal temporal trends in wave power stability in the Niger delta coast.

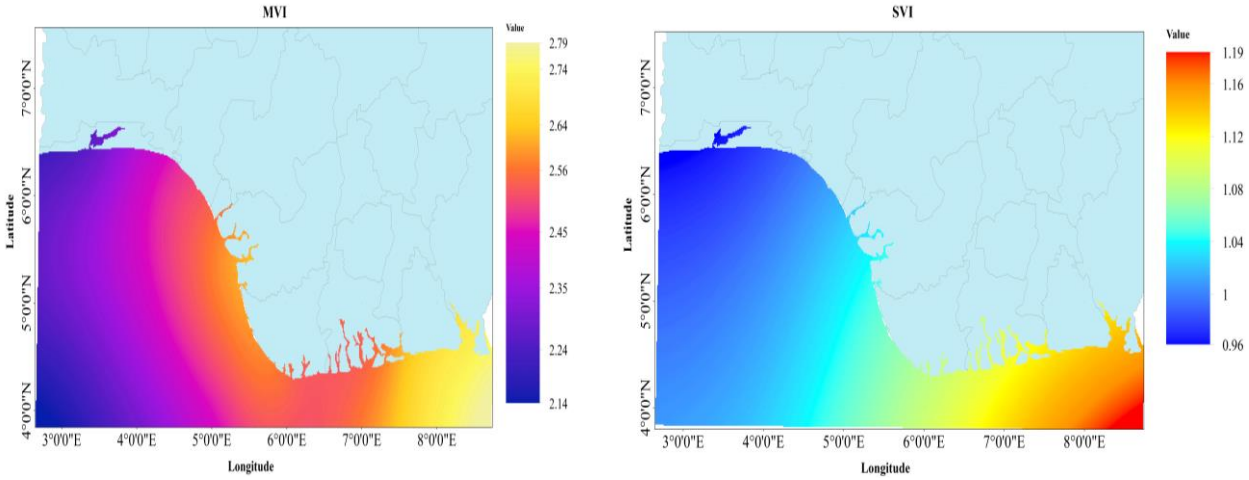

Figure 11. Spatial variation of wave power variability index in the Niger delta coast.

For both the MVI and SVI shown in figure. 11, the wave power stability increases west wards. It is particularly stable with MVI between 2.1 and 2.3 and SVI between 0.96 and 1.0 around Lagos Lagoon and southwards towards the western Gulf of Guinea. The variability indexes are larger and hence wave power is least stable in Ikpa Ibom IV with MVI between 2.7 and 2.79 and SVI between 1.14 and 1.185. For the variability indexes presented in figure. 12, wave power is most stable in year 1999 with values of 0.33 and 0.07 respectively for the MVI and SVI. For the MVI, least stability occurred in years 1989, 1995 and 2001 with values of 3.14, 3.1 and 3.19, while for the SVI, least stability occurred in years 1994 and 1995 with values of 1.25 and 1.28.

3.3.5. Bivariate Distribution of Wave Energy in the Niger Delta Coasts

Scatter table is frequently used to display the frequency of occurrence of sea states defined by a characteristic wave height (H_s) and wave period (T_e), [53].

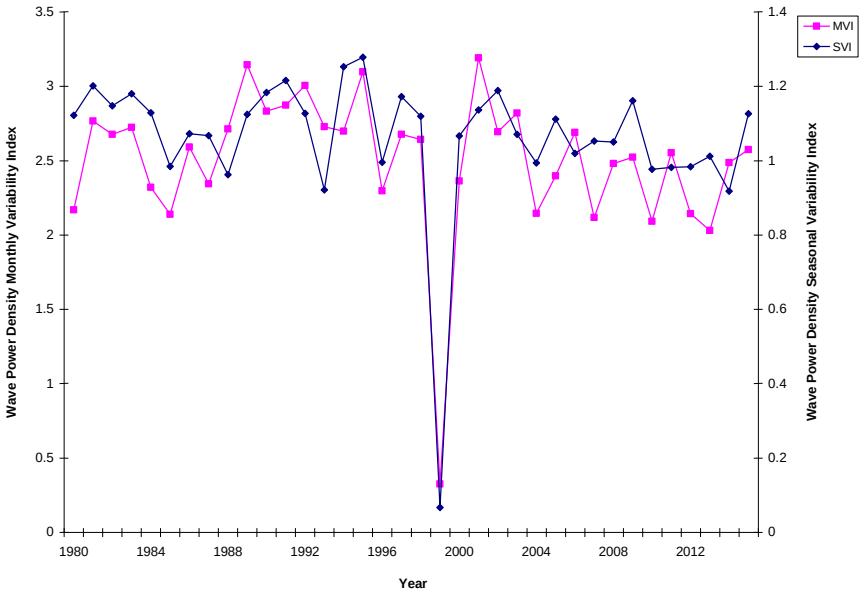

Figure 12. Temporal variation of wave power variability index in the Niger delta coast.

Table. 4 shows a bivariate distribution of significant wave height (H_s) and mean wave period (T_e) in the Niger delta coasts. It can be seen from the table that the most frequent sea states (bold and highlighted in green) concentrate between 2.5 s and 5 s for T_e and values ≤ 2. 5 m for H_s.

The total annual wave power for different sea states is presented in table. 5. It can be seen that the main wave energy **(**bold and highlighted in green**)** is also concentrated between 2.5 s and 5 s (T_e) and for values ≤ 2.5 m (H_s). When relating these results with the number of occurrences (Table. 4), it is observed that the most frequent sea states coincide with the most energetic sea states.

Table. 4. Number of occurrences of different sea states in the Niger delta coasts.

H_S/T_e	0-2.5	2.5-5	5-7.5	7.5-10	10-12.5	≥12.5
0-2.5	39353	1757390	44097	18	0	0
2.5-5	0	1	1	0	0	0
5-7.5	0	0	0	0	0	0
7.5-10	0	0	0	0	0	0
≥10.5	0	0	0	0	0	0

Table. 5. Total wave power (in GW/m) corresponding to sea states for different ranges of H_s and T_e in the mid Atlantic.

H_S/T_e	0-2.5	2.5-5	5-7.5	7.5-10	10-12.5	≥12.5
0-2.5	0.002	0.569	0.0175	7.E-9	0	0
2.5-5	0	0.0000154	0.0000155	0	0	0
5-7.5	0	0	0	0	0	0
7.5-10	0	0	0	0	0	0
≥10.5	0	0	0	0	0	0

4. Conclusions

This study evaluated the wind-wave energy resource over the Niger delta coasts using ERA Interim wind fields and a state-of-the-art spectral model, WW3. There is good agreement between measurements and simulations. The wind generally showed very poor characteristics. The annual mean WPD and wind speed over the location indicates that the region is poor for wind power applications. The shape parameter "k" showed that the wind is most stable in the month of August and least stable in October. Hence, August is most appropriate for the production of incessant and stable wind power. The scale parameter "c" showed that the wind power is most spread in August and least spread in November. Seasonal analysis indicates that the wind is more stable in winter and more spread during summer. The wind speed and WPD are highest in August and lowest in November. The wind is stronger in summer than in winter. Wind speed within the range of 0-4 m/s occurred most.

An analysis of the rich energy region revealed that no location in the Niger delta coasts is suitable for the exploitation of wave energy and in the establishment and design of wave energy converter systems. The spatial distribution of WPD is estimated, results showed that WPD intensifies westwards with maximum values ($70w/m^2$ - $86.5w/m^2$) distributed around Gulf of Guinea. The WPD generally showed declining trends for the year and seasons. The annual trend is -0.0021 w/m^2yr^{-1} while the trends at winter and summer are respectively -0.2107 w/m^2yr^{-1} and -0.362 w/m^2yr^{-1}. The annual mean wave power between 0.3kW/m and 0.61kW/m dominate most waters of the Niger delta, while lower values distribute in the rest regions. For the year and seasons, the wave power generally exhibits declining trends. The annual trend is -0.0029kW/myr^{-1} while the trends at winter and summer are respectively -0.0003 kW/myr^{-1} and -0.0048 kW/myr^{-1}. The wave power is minimum in the year 1999 with respective values of 0.039 kW/m and 0.038 kW/m for both the annual and summer averages. Largest wave power of 0.45 kW/m and 0.67 kW/m are seen in the year 1991. For the winter mean, highest wave power values of 0.16 kW/m, 0.15 kW/m, 0.16 kW/m and 0.17 kW/m are respectively found in the years 1980, 1988, 1992 and 2014, while least value of 0.04 kW/m is found in the year 1999.

Wave power stability intensifies westwards and most stable (COV of 1-1.1) around Lagos Lagoon. It is least stable (COV of 1.25-1.65) around Ikpa Ibom IV. The wave power stability exhibits declining trends of -0.0017, -0.0064 and -0.00008 respectively for the annual, winter and summer averages. The wave power is most stable in the year 1999 with COV ranging between 0.011 and 0.51. Also, the analysis of both the MVI and SVI showed that wave power stability increases west wards. The greatest stability is seen around Lagos Lagoon and southwards towards the western Gulf of Guinea with MVI between 2.1 and 2.3 and SVI between 0.96 and 1.0. The wave power is least stable in Ikpa Ibom IV with MVI between 2.7 and 2.79 and SVI between 1.14 and 1.185. The wave power is most stable in year 1999 with values of 0.33 and 0.07 respectively for the MVI and SVI.

The bivariate distribution of SWH (H_s) and Tm (T_e) revealed that the most frequent sea states concentrate between 2.5 s and 5 s for T_e and values $\leq$ 2. 5 m for H_s. Also, the analysis of total annual wave power for different sea states showed that the main wave energy is also concentrated between 2.5 s and 5 s (T_e) and for values $\leq$ 2.5 m (H_s).

References

[1] G. Besio, L. Mentaschi and A. Mazzino, Wave energy resource assessment in the Mediterranean Sea on the basis of a 35-year hindcast, Energy vol 94, pp. 50-63, 2016.

[2] A. M. Cornett, A global wave energy resource assessment. In: Proceedings of the eighteenth international offshore and polar engineering conference (ISOPE), International Society of Offshore and Polar Engineers, Paper No. ISOPE-2008-579. Vancouver, pp. 6-11, 2008.

[3] L. Hammar, J. Ehnberg, A. Mavumec, et al., Renewable ocean energy in the Western Indian Ocean, Renewable and Sustainable Energy Reviews, vol 16, pp. 4938-4950, 2012.

[4] M. Lopez, M. Veigas and G. Iglesias, On the wave energy resource of Peru, Energy Conversion and Management, vol 90, pp. 34-40, 2015.

[5] L. Rusu and F. Onea, Assessment of the performances of various wave energy converters along the European continental coasts, Energy, vol 82, pp. 889-904, 2015.

[6] K. Thomsen, Offshore Wind: A Comprehensive Guide to Successful Offshore Wind Farm Installation. Academic Press, London, UK, pp. 404, 2014.

[7] S. Astariz, C. Perez-Collazo, J. Abanades, et al., Co-located wave-wind farms: Economic assessment as a function of layout, Renewable Energy, vol 83, pp. 837-849, 2015.

[8] C. Perez-Collazo, D. Greaves and G. Iglesias, A review of combined wave and offshore wind energy, Renewable and Sustainable Energy Reviews, vol 42, pp. 141-153, 2015.

[9] L. Cradden, C. Kalogeri, I. M. Barrios, et al., Multi-criteria site selection for offshore renewable energy platforms, Renewable energy, vol 87, pp. 791-806, 2016.

[10] C. Maisondieu and M. Healy, The impact of the MARINET initiative on the development of Marine Renewable Energy, International Journal of Marine Energy, vol 12, pp. 77-86, 2015.

[11] L. Rusu and F. Onea, The performance of some state-of-the-art wave energy converters in locations with the worldwide highest wave power, Renewable and Sustainable Energy Reviews, vol 75, pp. 1348-1362, 2017.

[12] G. Emmanouil, G. Galanis, C. Kalogeri, et al., 10-year high resolution study of wind, sea waves and wave energy assessment in the Greek offshore areas, Renewable Energy, vol 90, pp. 399-419, 2016.

[13] S. Gallagher, R. Tiron, E. Whelan, et al., The near shore wind and wave energy potential of Ireland: a high resolution assessment of availability and accessibility, Renewable Energy, vol 88, pp. 494-516, 2016.

[14] C. Kalogeri, G. Galanis, C. Spyrou, et al., Assessing the European offshore wind and wave energy resource for combined exploitation, Renewable Energy, vol 101, pp. 244-264, 2017.

[15] M. Veigas, R. Carballo and G. Iglesias, Wave and offshore wind energy on an island, Energy for Sustainable Development, vol 22, pp. 57-65, 2014.

[16] E. D. Stoutenburg, N. Jenkins and M. Z. Jacobson, Power output variations of co-located offshore wind turbines and wave energy converters in California, Renewable Energy, vol 35(12), pp. 2781-2791, 2010.

[17] Ocean Energy Systems (OES) - International Energy Agency (IEA) Annual Report an Overview of Activities in 2017, 2017.

[18] T. Soukissian, F. Karathanasi and P. Axaopoulos, Satellite-Based Offshore wind resource assessment in the mediterranean sea, IEEE J. Ocean. Eng., vol 42, pp. 73-86, 2017.

[19] A. Energiewende and Sandbag, The European Power Sector in 2017 State of Affairs and Review of Current Developments Analysis. Available online at: https://sandbag.org.uk/wp/content/uploads/2018/01/EUpower-sector-report-2017.pdf, 2018.

[20] F. Onea, S. Ciortan and E. Rusu, Assessment of the potential for developing combined wind-wave projects in the European nearshore. Energy Environ., vol 28, pp. 580-597, 2017.

[21] D. McMillan and G.W. Ault, Techno-economic comparison of operational aspects for direct drive and gearbox-driven wind turbines. IEEE Trans. Energy Convers., vol 25, pp. 191-198, 2010.

[22] Y. Liu, Y. Li, F. He and H. Wang, Comparison study of tidal stream and wave energy technology development between China and some Western Countries, Renew. Sustain. Energy Rev., vol 76, pp. 701-716, 2017.

[23] F. Fusco, G. Nolan and J.V. Ringwood, Variability reduction through optimal combination of wind/wave resources - an Irish case study. Energy, vol 35, pp. 314-325, 2010.

[24] M. Veigas and G. Iglesias, Wave and offshore wind potential for the island of Tenerife. Energy Convers. Manage., vol 76, pp. 738-745, 2013.

[25] M. Veigas and G. Iglesias, A hybrid wave-wind offshore farm for an island, Int. J. Green Energy, vol 12, pp. 570-576, 2015.

[26] M. Veigas, R. Carballo and G. Iglesias, Wave and offshore wind energy on an island, Energy Sustain. Dev., vol 22, pp. 57-65, 2014.

[27] M. Veigas, V. Ramos and G. Iglesias, A wave farm for an island: detailed effects on the nearshore wave climate. Energy, vol 69, pp. 801-812, 2014.

[28] Z. Gao, T. Moan, L. Wan and M. Constantine, Comparative numerical and experimental study of two combined wind and wave energy concepts, J. Ocean Eng. Sci., vol 1, pp. 36-51, 2016.

[29] M. Karimirad and K. Koushan, Wind WEC: combining wind and wave energy inspired by hywind and wavestar, in Proceedings of the International Conference on Renewable Energy Research and Applications, (Birmingham), 2016.

[30] A. Azzellino, V. Ferrante, J.P. Kofoed, C. Lanfrediand and D. Vicinanza, Optimal siting of offshore wind-power combined with wave energy through a marine spatial planning approach, Int. J. Mar. Energy, pp. 3-4, 2013.

[31] C. Perez-Collazo, M.M. Jakobsen, H. Buckland and J. Fernández-Chozas, Synergies for a Wave-Wind Energy Concept, Frankfurt: EWEA, 2013.

[32] S. Astariz and G. Iglesias, Selecting optimum locations for co-located wave and wind energy farms. Part I: The Co-Location Feasibility index, Energy Conversion Manage. vol 122, pp. 589-598, 2016.

[33] S. Astariz and G. Iglesias, The collocation feasibility index - A method for selecting sites for co-located wave and wind farms, Renew. Energy, vol 103, pp. 811-824, 2017.

[34] S. Astariz, A.J. Perez-Collazo and G. Iglesias, Hybrid wave and offshore wind farms: a comparative case study of co-located layouts, Int. J. Marine Energy, vol 15, pp. 2-16, 2016.

[35] C. Pérez-Collazo, D. Greaves and G. Iglesias, A review of combined wave and offshore wind energy, Renew. Sustain. Energy Rev., vol 42, pp. 141-153, 2015.

[36] L. Margheritini, A. M. Hansen and P. Frigaard, A method for EIA scoping of wave energy converters-based on classification of the used technology, Environ. Impact Assess. Rev., vol 32, pp. 33-44, 2012.

[37] H. Bailey, K. L. Brookes and P. M. Thompson, Assessing environmental impacts of offshore wind farms: lessons learned and recommendations for the future, Aquatic Biosyst, vol 10(8), 2014.

[38] L. Riefolo, C. Lanfredi, A. Azzellino, D. Vicinanza, G.R. Tomasicchio, F. D'Alessandro, et al., Offshore wind turbines: an overview of the effects on the marine environment, in ISOPE International Society Of Offshore And Polar Engineers Rhodes (Rodos), pp. 427-434, 2016.

[39] H. L. Tolman, User manual and system documentation of Wavewatch-III version 3.14. NOAA/NWS/ NCEP Technical Note (276), 194, 2009.

[40] D. S. Wilks, Statistical Methods in the Atmospheric Sciences: An Introduction. Academic Press, San Diego, Calif, USA, 1995.

[41] I. Fyrippis, P. J. Axaopoulos and G. Panayiotou, Wind energy potential assessment in Naxos Island, Greece. Appl Energy, vol 87(2), pp. 577-86, 2010.

[42] O. Ohunakin, M. Adaramola and O. Oyewola, Wind energy evaluation for electricity generation using WECS in seven selected locations in Nigeria, Appl Energy, vol 88(9), pp. 3197-206, 2011.

[43] M. Gökçek, A. Bayülken and S. Bekdemir, Investigation of wind characteristics and wind energy potential in Kirklareli, Turkey, Renewable Energy, vol 32(10), pp. 1739-52, 2007.

[44] C. Justus, W. Hargraves, A. Mikhail and D. Graber, Methods for estimating wind speed frequency distributions. J Appl Meteorol, vol 17(3), pp. 350-3, 1978.

[45] S. A. Akdag and A. Dinler, A new method to estimate Weibull parameters for wind energy applications, Energy Convers Manage, vol 50(7), pp. 1761-6, 2009.

[46] M. Stevens and P. Smulders, The estimation of the parameters of the Weibull wind speed distribution for wind energy utilization purposes, Wind Eng., vol 3, pp. 132-45, 1979.

[47] H. Rinne, The Weibull distribution: a handbook. CRC Press, 2010.

[48] J. K. Khan, F. Ahmed, Z. Uddin, S. T. Iqbal, U. J. Saif, A. A. Siddiqui and A. Aijaz, Determination of Weibull Parameter by four Numerical Methods and Prediction of Wind Speed in Jiwani (Balochistan), J Basic Appl Sci, vol 11, pp. 62-68, 2015.

[49] H. Saleh, A. Abou El-Azm Aly and S. Abdel-Hady, Assessment of different methods used to estimate Weibull distribution parameters for wind speed in Zafarana wind farm, Suez Gulf, Egypt, Energy, vol 44(1), pp. 710-9, 2012.

[50] J. F. Manwell, J. G. McGowan and A. L. Rogers, Wind energy explained: theory, design and application, Amherst (USA). John Wiley & Sons, 2002.

[51] M. Sathyajith, Wind energy: fundamentals, resource analysis and economics, Springer, 2006.

[52] G. Iglesias and R. Carballo, Choosing the site for the first wave farm in a region: A case study in the Galician Southwest (Spain), Energy, vol 36(9), pp. 5525-5531, 2011.

[53] A. Vosough, Wave power, Int. J. Multidiscip. Sci. Eng., vol 2(7), pp. 60-63, 2011.

[54] C. W. Zheng, L. Zhou, B. K. Jia, J. L. Pan and X. Li, Wave characteristic analysis and wave energy resource evaluation in the China Sea, Journal of Renewable and Sustainable Energy, vol 6, 2014.

[55] D. Elliott and M. Schwartz, Wind energy potential in the United States, Richland, WA: Pacific Northwest Laboratory PNL-SA-23109, 1993.